

Far-field optical nanoscopy with reduced number of state transition cycles

Thorsten Staudt,^{1,2,4} Andreas Engler,^{2,4} Eva Rittweger,^{1,2} Benjamin Harke,^{1,3}
Johann Engelhardt,² and Stefan W. Hell^{1,2,*}

¹Max Planck Institute for Biophysical Chemistry, Am Fassberg 11, 37077 Göttingen, Germany

²German Cancer Research Center / BioQuant, Im Neuenheimerfeld 267, 69120 Heidelberg, Germany

³Currently with the Italian Institute of Technology, Via Morego 30, 16163 Genova, Italy

⁴these authors contributed equally to this work

*shell@gwdg.de

Abstract: We report on a method to reduce the number of state transition cycles that a molecule undergoes in far-field optical nanoscopy of the RESOLFT type, i.e. concepts relying on saturable (fluorescence) state transitions induced by a spatially modulated light pattern. The method is exemplified for stimulated emission depletion (STED) microscopy which uses stimulated emission to transiently switch off the capability of fluorophores to fluoresce. By switching fluorophores off only if there is an adjacent fluorescent feature to be recorded, the method reduces the number of state transitions as well as the average time a dye is forced to reside in an off-state. Thus, the photobleaching of the sample is reduced, while resolution and recording speed are preserved. The power of the method is exemplified by imaging immunolabeled glial cells with up to 8-fold reduced photobleaching.

©2011 Optical Society of America

OCIS codes: (180.1790) Confocal microscopy; (180.2520) Fluorescence microscopy; (230.1040) Acousto-optical devices; (350.5730) Resolution.

References and links

1. S. W. Hell, and J. Wichmann, "Breaking the diffraction resolution limit by stimulated emission: stimulated-emission-depletion fluorescence microscopy," *Opt. Lett.* **19**(11), 780–782 (1994).
2. T. A. Klar, S. Jakobs, M. Dyba, A. Egner, and S. W. Hell, "Fluorescence microscopy with diffraction resolution barrier broken by stimulated emission," *Proc. Natl. Acad. Sci. U.S.A.* **97**(15), 8206–8210 (2000).
3. E. Betzig, G. H. Patterson, R. Sougrat, O. W. Lindwasser, S. Olenych, J. S. Bonifacino, M. W. Davidson, J. Lippincott-Schwartz, and H. F. Hess, "Imaging Intracellular Fluorescent Proteins at Nanometer Resolution," *Science* **313**(5793), 1642–1645 (2006).
4. M. J. Rust, M. Bates, and X. W. Zhuang, "Sub-diffraction-limit imaging by stochastic optical reconstruction microscopy (STORM)," *Nat. Methods* **3**(10), 793–796 (2006).
5. S. T. Hess, T. P. K. Girirajan, and M. D. Mason, "Ultra-high resolution imaging by fluorescence photoactivation localization microscopy," *Biophys. J.* **91**(11), 4258–4272 (2006).
6. S. W. Hell, "Far-Field Optical Nanoscopy," *Science* **316**(5828), 1153–1158 (2007).
7. S. W. Hell, "Microscopy and its focal switch," *Nat. Methods* **6**(1), 24–32 (2009).
8. S. Hell, "Far-Field Optical Nanoscopy," in *Single Molecule Spectroscopy in Chemistry*, A. Gräslund, Rigler, R., Widengren, J., ed. (Springer, Berlin, 2009), pp. 365 - 398.
9. S. E. Irvine, T. Staudt, E. Rittweger, J. Engelhardt, and S. W. Hell, "Direct light-driven modulation of luminescence from Mn-doped ZnSe quantum dots," *Angew. Chem. Int. Ed. Engl.* **47**(14), 2685–2688 (2008).
10. E. Rittweger, K. Y. Han, S. E. Irvine, C. Eggeling, and S. W. Hell, "Sted microscopy reveals crystal colour centres with nanometric resolution," *Nat. Photonics* **3**(3), 144–147 (2009).
11. P. S. Dittrich, and P. Schwill, "Photobleaching and stabilization of fluorophores used for single-molecule analysis with one- and two-photon excitation," *Appl. Phys. B* **73**(8), 829–837 (2001).
12. L. L. Song, C. A. Varma, J. W. Verhoeven, and H. J. Tanke, "Influence of the triplet excited state on the photobleaching kinetics of fluorescein in microscopy," *Biophys. J.* **70**(6), 2959–2968 (1996).
13. J. Vogelsang, R. Kasper, C. Steinhauer, B. Person, M. Heilemann, M. Sauer, and P. Tinnefeld, "A Reducing and Oxidizing System Minimizes Photobleaching and Blinking of Fluorescent Dyes," *Angew. Chem. Int. Ed. Engl.* **47**(29), 5465–5469 (2008).
14. G. Donnert, J. Keller, R. Medda, M. A. Andrei, S. O. Rizzoli, R. Luhrmann, R. Jahn, C. Eggeling, and S. W. Hell, "Macromolecular-scale resolution in biological fluorescence microscopy," *Proc. Natl. Acad. Sci. U.S.A.* **103**(31), 11440–11445 (2006).

15. R. A. Hoebe, C. H. Van Oven, T. W. J. Gadella, P. B. Dhonukshe, C. J. F. Van Noorden, and E. M. M. Manders, "Controlled light-exposure microscopy reduces photobleaching and phototoxicity in fluorescence live-cell imaging," *Nature Biotechnol.* **25**, 249–253 (2007).
16. S. W. Hell, "Toward fluorescence nanoscopy," *Nat. Biotechnol.* **21**(11), 1347–1355 (2003).
17. V. Westphal, and S. W. Hell, "Nanoscale Resolution in the Focal Plane of an Optical Microscope," *Phys. Rev. Lett.* **94**(14), 143903 (2005).
18. B. Härke, J. Keller, C. K. Ullal, V. Westphal, A. Schoenle, and S. W. Hell, "Resolution scaling in STED microscopy," *Opt. Express* **16**(6), 4154–4162 (2008).
19. C. G. Dotti and K. Simons, "Polarized Sorting of viral glycoproteins to the axon and dendrites of hippocampal neurons in culture," *Cell* **62**, 63–72 (1990).
20. M. Encinas, M. Iglesias, Y. H. Liu, H. Y. Wang, A. Muhaisen, V. Cena, C. Gallego, and J. X. Comella, "Sequential treatment of SH-SY5Y cells with retinoic acid and brain-derived neurotrophic factor gives rise to fully differentiated, neurotrophic factor-dependent, human neuron-like cells," *J. Neurochem.* **75**(3), 991–1003 (2000).
21. S. Back, P. Haas, J. A. Tschaepé, T. Gruebl, J. Kirsch, U. Mueller, K. Beyreuther, and S. Kins, "beta-amyloid precursor protein can be transported independent of any sorting signal to the axonal and dendritic compartment," *J. Neurosci. Res.* **85**(12), 2580–2590 (2007).
22. S. W. Hell, and M. Kroug, "Ground-state depletion fluorescence microscopy, a concept for breaking the diffraction resolution limit," *Appl. Phys. B* **60**(5), 495–497 (1995).
23. S. Bretschneider, C. Eggeling, and S. W. Hell, "Breaking the diffraction barrier in fluorescence microscopy by optical shelving," *Phys. Rev. Lett.* **98**(21), 218103 (2007).
24. R. Heintzmann, T. M. Jovin, and C. Cremer, "Saturated patterned excitation microscopy--a concept for optical resolution improvement," *J. Opt. Soc. Am. A* **19**(8), 1599–1609 (2002).
25. M. G. L. Gustafsson, "Nonlinear structured-illumination microscopy: wide-field fluorescence imaging with theoretically unlimited resolution," *Proc. Natl. Acad. Sci. U.S.A.* **102**(37), 13081–13086 (2005).
26. R. Heintzmann, and M. G. L. Gustafsson, "Subdiffraction resolution in continuous samples," *Nat. Photonics* **3**(7), 362–364 (2009).
27. H. Bock, C. Geisler, C. A. Wurm, C. Von Middendorff, S. Jakobs, A. Schonle, A. Egner, S. W. Hell, and C. Eggeling, "Two-color far-field fluorescence nanoscopy based on photoswitchable emitters," *Appl. Phys. B* **88**(2), 161–165 (2007).
28. J. Fölling, M. Bossi, H. Bock, R. Medda, C. A. Wurm, B. Hein, S. Jakobs, C. Eggeling, and S. W. Hell, "Fluorescence nanoscopy by ground-state depletion and single-molecule return," *Nat. Methods* **5**(11), 943–945 (2008).
29. S. W. Hell, "Strategy for far-field optical imaging and writing without diffraction limit," *Phys. Lett. A* **326**(1–2), 140–145 (2004).

1. Introduction

Far-field fluorescence microscopy with conceptually diffraction-unlimited spatial resolution, i.e. far-field fluorescence nanoscopy, has made substantial advancements in recent years, demonstrating its capability in a number of variants [1–5]. To overcome the diffraction limit, the modern fluorescence nanoscopy techniques of high practical relevance exploit two distinguishable states of the marker molecules, usually a fluorescent 'on' (bright) and a non-fluorescent 'off' (dark) state. Sequentially transferring fluorophores that are closer than the diffraction barrier between these states enables the discrimination of features that are closer than half the wavelength of light [6]. More precisely, dark to bright state transitions are implemented in such a way that all the features exposed to the (inevitably diffracted) excitation light do not respond with fluorescence, with the exception of the feature or molecule that is to be registered.

In methods based on a coordinate-targeted readout mode, i.e. on the nanoscopy types relying on reversible saturable and switchable fluorescence transitions (RESOLFT), such as stimulated emission depletion (STED) microscopy, the spatial coordinate at which the markers are able to fluoresce (i.e. are 'on') is predefined by the location of the intensity minimum of the light pattern driving the on-off transition [6, 7]. Thus, the coordinates of the signaling and non-signaling fluorophores are predefined in space. These coordinate intervals can be as small as a molecule. The molecules outside these predefined 'on' or 'off' state coordinates are forced to be 'off' or 'on' respectively, whereby 'off' means incapable of emitting relevant fluorescence photons when exposed to excitation light. The image is gained by translating the beams through the specimen, thus altering the coordinate in which the molecules are 'on' and the fluorescence is registered [6, 7].

However, because of this light induced change in fluorescence capability, the fluorophores are forced to undergo numerous transitions between bright and dark states during recording

[6, 7]. The higher the gain in resolution is, the finer the spatial discrimination between the two states has to be, and the larger the number of cycles becomes that a molecule has to undergo during imaging. For example, in a standard scanning procedure, whereby the on-off switching beam featuring a zero (e.g. the STED beam) linearly progresses across the specimen, a resolution increase by m -fold over the diffraction barrier in the x -, and y -directions of the focal plane roughly entails $m \times m$ switching cycles. $m \times m \times m$ cycles are needed if the same resolution increase is to be gained along the optic axis (z) as well [8]. Scanning with stripes ('structured illumination') also entails multiples of m of on-off cycles. This assessment applies if a single switching cycle is used per subdiffraction-sized pixel. The numbers may be larger if the wavelengths used for fluorescence generation also induce on-off transitions, i.e. if there is an action cross-talk of the light beams used.

Unfortunately, imposing frequent state transitions on a marker molecule increases its probability to end up in a long-lived dark state, arresting the crucial on-off transitions. As a result, the fluorophore cannot contribute to the image formation any longer; it is bleached or at least appears to be 'bleached' on the recording time scale. Therefore, ensuring that the marker is able to switch repeatedly between the fluorescence on and off states is key to subdiffraction imaging in the RESOLFT mode. By contrast, for nanoscopy techniques based on stochastic single molecule read out, one full on-off switching cycle is sufficient to record an image since each fluorophore needs to be switched (on and off) and localized only once [6, 7].

Many switching events can be accommodated in the process by choosing photostable fluorophores such as special quantum dots or color centers in diamond. These exceptional fluorophores allow more than thousand [9] or a nearly unlimited number of on-off cycles [10]. However, most dyes or fluorescent proteins used for biolabeling, especially those realizing the on-off transition by photoisomerization or other alterations of the chemical structure and conformation, can accommodate only $\ll m \times m$ numbers on-off cycles. Switching fatigue darkens the fluorophores on the time scale of measurement.

Apart from selecting molecules with comparatively little switching fatigue, two further strategies can be pursued in order to foster the on-off switching ability of the marker. The first one is to stabilize the molecule chemically, i.e. adapt the chemical environment to prevent any detrimental chemical reaction following the optically induced state transition. To increase the number of state transitions a dye is able to cope with, previous work aimed at avoiding long-lived dark states by adding anti-bleaching agents [11–13]. However, these approaches are not compatible with living cells and have to be adapted to the dyes employed. The second strategy interrupts unnecessary illumination of molecules residing in a photoabsorbing dark state or triplet state leading to chemical reactions. Referred to as D-REX and T-REX [14], respectively, these methods allow the molecules residing in these states to relax to the non-reactive ground state, by ensuring that the time span between consecutive photon absorptions is long enough for the dark states to decay. However, since the triplet lifetimes are quite long (microseconds), the photon absorption rates have to be < 1 MHz or lower, which either lengthens the recording time or requires very fast scanning. Besides, T- or D-Rex strategies do not prevent bleaching pathways associated with short-lived states, such as those emanating from excited singlet states.

Therefore, the approach presented here aims at minimizing the time a fluorophore is, on average, optically forced to reside in either the 'on' or the 'off' state (depending on the on-off molecular mechanism employed) by the way the time-sequential coordinate-targeted readout (i.e. the scanning) of the object is implemented. This method also eliminates unnecessary on-off cycles of the dye thus concomitantly reducing the overall light dose and photostress.

The approach relies on the insight that the only role of the on-off transition in subdiffraction far-field imaging is to make features residing within subdiffraction distances different [1, 6, 7]. For this reason, the on-off transition should be enforced only if adjoining features need to be separated. If no separation is needed, there is no need for inducing an on-off-transition or for maintaining the on-off gradient of states at subdiffraction scales. To this end, an intelligent on-off switching and light exposure scheme is put into practice which stalls the on-off switching when there is no feature to be discriminated from other features residing

within the diffraction region. Our strategy is related to that by Manders et al [15] who have introduced a scheme called CLEM for increasing the number of detected fluorescence photons in scanning microscopy. In our case, the net effect is that the number of unnecessary on-off state transitions is reduced without any trade-offs in resolution, signal to noise ratio, or imaging speed. Actually, the introduced modality also implies an acceleration of the recording time. It is applicable, with some adaptations, for all nanoscopy techniques based on a coordinate-targeted readout mode. Here we demonstrate this approach exemplarily for STED microscopy, which is currently the most widely employed targeted switching (i.e. RESOLFT type) nanoscopy method.

2. Materials and methods

2.1 Reduction of state transition cycles (RESCue-)STED

The scanning modality suitable for reducing the overall number of state transitions inside a three dimensional (3D) specimen is readily found when considering how the coordinate targeted nanoscopy modality operates. The optical transitions between the bright and the dark states ensure that the markers in the focal region are kept non-responsive to the excitation light except those located at the coordinate which is to be read out (Fig. 1a). The coordinate range at which the fluorophores are allowed to respond by fluorescence emission is given by $\Delta r \approx \lambda / (2n \sin \alpha \sqrt{1 + I/I_s})$, with the maximum intensity I bordering the local intensity minimum (zero) driving the on-off transition [10, 16, 17]. I_s is the threshold intensity at which $> 50\%$ of the molecules have undergone the transition, λ is the wavelength of light and $n \sin \alpha$ the numerical aperture of the lens. Δr also corresponds to the resolution attainable for a given intensity I . Separation at the subdiffraction level works by discriminating the features or molecules residing right outside the subdiffraction coordinate range Δr ; the beam inducing the on-off transition switches the fluorescence capability of these dyes off.

For example, in a STED microscope employing a doughnut-shaped STED beam, the targeted coordinate is the region of extent Δr close to the central zero of the doughnut. However, if there is no molecule at this coordinate, there is no reason for (time-extended) switching off the fluorophores located outside this region. More generally speaking, there is no need to switch off the fluorophores located within the diffraction area with $\sim \lambda / 2n \sin \alpha$ extent. To make a decision whether it is needed to (extensively) switch those fluorophores off, we determine the number of photons originating from the subdiffraction region $\Delta r \approx \lambda / (2n \sin \alpha \sqrt{1 + I/I_s})$ in which fluorescence is allowed. We make this decision within the decision time dT which is a small fraction of the pixel dwell time pT . In case that this number is below a certain lower threshold (lTh), a binary decision can be made on whether an object is present within $\Delta r \approx \lambda / (2n \sin \alpha \sqrt{1 + I/I_s})$. With no fluorescent features at this location, an exposure to light, in particular an optically induced off-switching of the neighboring molecules, would be meaningless in the best, but highly unfavorable in the worst case. Therefore the illumination of both the excitation and the suppression beam is stopped for the residual time of pT . Alternatively, the translation of the minimum could proceed to the next detection coordinate range yielding shorter acquisition times. How many excitation/de-excitation transitions in percentage can be avoided in STED microscopy due to lTh depends on pT/dT , the fluorescence distribution, and on the ratio between the (3D-) extent of the diffraction zone and the subdiffraction resolution, i.e. on $\sqrt{1 + I/I_s}$. Increased resolution, i.e. decreased Δr , enables a more accurate spatial discrimination of the fluorophores (Fig. 1b). Only if an object is present within the reduced spatial range in which fluorescence is allowed, the light inducing the on-off transition as well as the fluorescence read-out remains on.

Another strategy for reducing the numbers of state transitions is to halt the beam exposure if the desired signal to noise ratio (SNR) is reached, meaning that an upper threshold (uTh) of

detected photons is specified. In case uTh is reached in a time rT (read out time) shorter than the dwell time pT , the illumination is stopped, thus preventing unnecessary transitions at positions with high fluorophore density. In this case, the photon counts are corrected by the factor pT/rT to account for the shortened measuring time. The reduction of state transition cycles due to uTh depends on pT/rT and also on the fluorescence distribution as well as on the resolution increase factor. The relevance of this parameter is most pronounced for bright and dense samples.

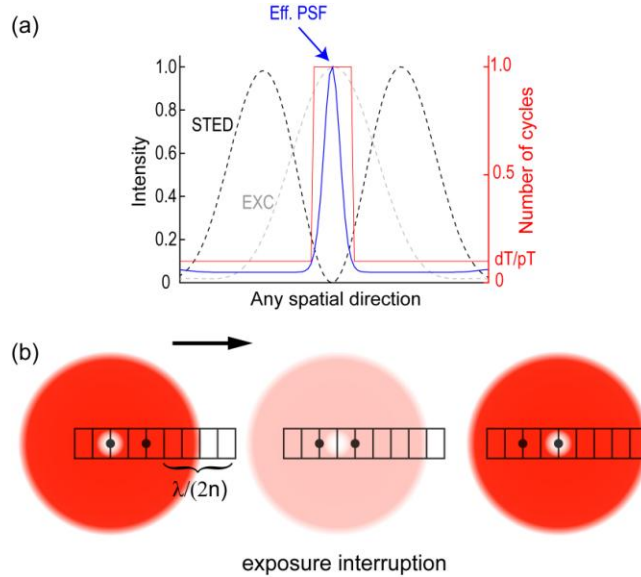


Fig. 1. Exposure decision-making process for RESCue-STED. a) The role of the doughnut-shaped STED beam is to switch off the fluorescence capability of molecules or features residing within the diffraction barrier, so that the ones located at about the doughnut zero are allowed to emit and hence be registered independently from their neighbors right outside the ‘fluorescence-allowed’ region. The effective PSF (blue line) describes the region in which the molecules can fluoresce. The red line illustrates the reduced number of transition cycles through RESCue with $dT/pT = 0.1$. The idea behind RESCue-STED is to avoid extended optical forcing of molecules to reside in the ground (off) state by stimulated emission if there is no feature or molecule to be recorded within the subdiffraction sized region given by the effective PSF. b) Two objects falling within subdiffraction distances are separated by switching the fluorescence of one of them off; here this is accomplished by the red doughnut-shaped STED beam (large red circle). If no fluorescent feature is present within the subdiffraction fluorescence area (small white circle), the optical beams can be interrupted, because there is no need for the STED beam to switch off features for separation. In this way the number of state transition cycles and hence the bleaching probability is reduced. Grey circles indicate fluorophores. The grid marks the pixels.

Note that in the case of fluorophores undergoing a reversible switch to a metastable dark state, such as a triplet state in GSD microscopy, or between a cis-trans state pair as in the RESOLFT concept operating with reversibly photoactivatable fluorophores, the number of state transitions is generally lower than in STED microscopy. This is because in some cases fluorophores residing in the metastable dark state may not absorb photons of the wavelengths in use, thus reducing the total number of optically induced state transition. In STED microscopy the number of state transitions is higher, because both signal generation and on-off-switching occurs just between two states, i.e. the ground and the fluorescent state. The role of the excitation beam is two-fold: switching-on and reading out. In contrast, when using reversibly switchable fluorophores, these two actions can be disentangled, because switching-on, switching-off, and fluorescence generation can in principle require distinct wavelengths.

2.2 Optical setup used for the Nile Red and Atto565 experiments

Excitation at 532 nm was realised using a pulsed laser diode (PicoTA, Picoquant, Berlin, Germany) which was triggered by the STED pulses at 647 nm via a photodiode (Alphaslas, Göttingen, Germany) which were generated by an actively mode locked (APE, Berlin, Germany) Ar-Kr laser (Spectra Physics-Division of Newport Corporation, Irvine, USA). The synchronized pulses were combined using acousto-optical tunable filters (AOTF) (Crystal Technologies, Palo Alto, USA) and coupled into a microscope (DMI 4000B with an objective lens ACS APO 63x/1.3NA, Leica Microsystems GmbH, Mannheim, Germany) equipped with a three axis piezo stage-scanner (PI, Karlsruhe, Germany) which also imaged the fluorescence signal onto a confocally arranged aperture of a photon counting module (SPCM-AQR-13-FC, PerkinElmer, Canada). The AOTFs also served as fast shutters and independent power controllers for each laser beam as well as a filter system selecting the fluorescence signal. For additional filtering, a band-pass filter (580/40, AHF Analysentechnik, Tübingen, Germany) was used. The doughnut-shaped intensity profile of the STED focus was generated by inserting a glass phase plate (RPC Photonics, NY, USA) which induced a helical phase ramp from 0 to 2π on the initially flat wave front.

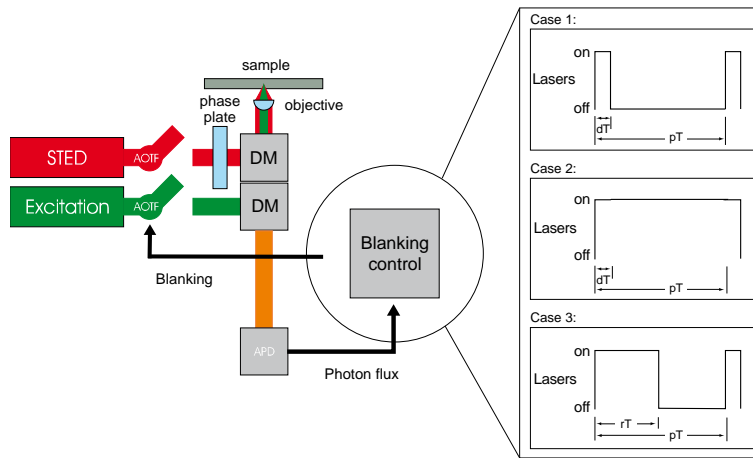


Fig. 2. Setup for RESCue-STED (left side). AOTFs are added to the STED microscope which are used to switch both laser beams on and off during the RESCue experiments depending on the measured fluorescence photon flux at each position in the sample. Three cases have to be considered (right side): Case 1: The lower threshold is not reached during the decision time dT (no fluorescent object is present in the reduced STED focus). The lasers are switched off during the dwell time pT . Case 2: The lTh is reached during dT (a fluorescent object is present in the effective STED focus). The lasers remain switched on during pT . Case 3: The lower and the upper threshold uTh is reached during the dT and the readout time rT respectively (a bright object is detected). The lasers are switched off after a certain number of photons are collected according to uTh . DM: dichroic mirror.

2.3 Optical setup used for the 3D experiments using Atto647N

A similar setup has been described by Harke et al [18]. The excitation pulses were provided by a 635 nm laser diode which was triggered by the STED pulses at 750 nm of a Ti:Sapphire laser. Both beams were focused by an oil immersion lens (Plan APO, 100x/1.4NA, Leica Microsystems GmbH, Mannheim, Germany) which was also used to collect the fluorescence signal. A phase plate retarding the inner circle of the STED beam by π was inserted to generate an intensity profile in the focus featuring a central zero with a strong gradient in the axial and a weak gradient in the lateral direction providing 3D resolution enhancement. For detection four photon-counting avalanche photodiodes (APD) (PerkinElmer, Canada) were used which reduce saturation effects appearing with a single APD. As fast shutters an EOM (LM002 P5W, Linos, Germany) and an AOTF (AA Opto-Electronic, Orsay Cedex, France)

were used in the STED and excitation beams, respectively. Both devices were controlled by a home built circuit board described below.

2.4 Implementation of RESCue

The ITh is implemented by a stand-alone circuit board, which utilizes a counter to track the photons at the detector synchronized with the pixel clock. This information is then used as binary decision for the blanking devices (AOTF) to switch both the excitation and the STED beams. A field programmable gate array (FPGA, National Instruments, Austin, USA) is utilized to implement both RESCue parameters (lTh and uTh). It was programmed such that the lasers are switched off if the lTh is not reached and when the uTh is reached. rT is recorded to correct for the shortened measuring time. The FPGA also controls the scanning electronics. The FPGA allows adaptive changes of the RESCue parameters lTh, uTh, and dT within the scan loops based on the information gained in previous scans or depending on algorithms to match the changed specimen and fluorescence properties. The parameters lTh, uTh, dT should be chosen to obtain maximal bleaching reduction without affecting image quality. If the value for lTh is set too low, there is hardly any effect. If it is set too high, dim objects may be overlooked. dT has to be long enough to allow a reliable decision making about whether an object of interest is present in the reduced fluorescence volume or not. Finally, the parameter uTh should be chosen depending on the desired SNR.

2.5 Cell culture and immunocytochemistry

Glioblastoma: GFAP

For immunocytochemistry, the U373 glioblastoma cells were seeded on standard glass coverslips to a confluency of 50-80% and permeabilized with cold methanol (-20°C) for 4-6 min. The cells were subsequently washed in PBS with 1% BSA (blocking buffer) and incubated with primary antibodies (anti GFAP mouse IgG, Sigma, Germany). After 1 h of incubation, the cells were washed with blocking buffer for 10 min and incubated with secondary antibodies (Atto565 goat anti-mouse IgG) for 1 h after the protocol from Molecular Probes, Carlsbad. For imaging, the cells were mounted in Mowiol (Sigma, Germany) containing DABCO (Sigma, Germany) as an antioxidant.

APP: primary mouse neurons (DIV8)

Embryos (E14) from wt (C57BL/6NCrI; Charles River) mice were separated; dissociated mixed cortical neuron cultures were prepared as described previously [19]. Neurons were grown on poly-L-lysine-coated 15-mm coverslips (Marienfeld, Germany) in serum-free Neurobasal Media (Gibco, Germany) with B-27 supplement (Gibco, Germany), 25 μM glutamate (Sigma, Germany), and 0.5 mM glutamine (Sigma, Germany). For immunocytochemical analysis, primary neurons were fixed with 4% PFA (Sigma, Germany) and permeabilized 10 min with 0.1% NP-40/Nonidet (Fluka, Germany) in PBS. Cells were incubated with primary antibody (monoclonal anti-APP-antibody 4G8 (Chemicon, CA) diluted in 5% goat serum in PBS) at 4°C overnight, washed with PBS, incubated with secondary antibody (Atto565 goat anti-mouse IgG, 10 $\mu\text{g}/\text{ml}$), and embedded in Mowiol (Sigma, Germany) on glass coverslips.

Neuroblastoma: Lamin

The SH-SY5Y neuroblastoma cell line was grown as described previously [20]. Cells were seeded on standard glass coverslips to a confluency of about 80%. For immunostaining of the nuclear lamina, the cells were fixed with 3.7% PFA for 15 min followed by a 5 min-treatment with Triton X-100. Before the incubation with the primary antibody, the cells were blocked in 1% BSA in PBS for 5 min. Anti-lamin B1 rabbit IgG (Abcam, Cambridge, UK) was used as primary antibody, anti-rabbit conjugated Atto647N IgG as secondary antibody respectively. Both antibodies were diluted in blocking buffer. Postfixation was carried out with 3.7% PFA for 10 min. Cells were mounted in Mowiol.

Fluorescent bead sample preparation

We sowed the Nile Red filled polystyrene microspheres (diameter, 21 nm; 2% solids in distilled water; Molecular Probes) on poly-L-lysine (Sigma, Germany) coated coverslips and mounted them in DABCO containing Mowiol (Sigma, Germany) to avoid diffusion.

3. Results

To exemplify the power of RESCue we measured different samples under the application of RESCue-STED with different settings compared to standard STED imaging. In the following measurements the fluorescence signal of a confocal pre- and post-scan are evaluated to define a bleaching factor. This factor is determined by the total fluorescence signal in the pre scan divided by that in the post scan.

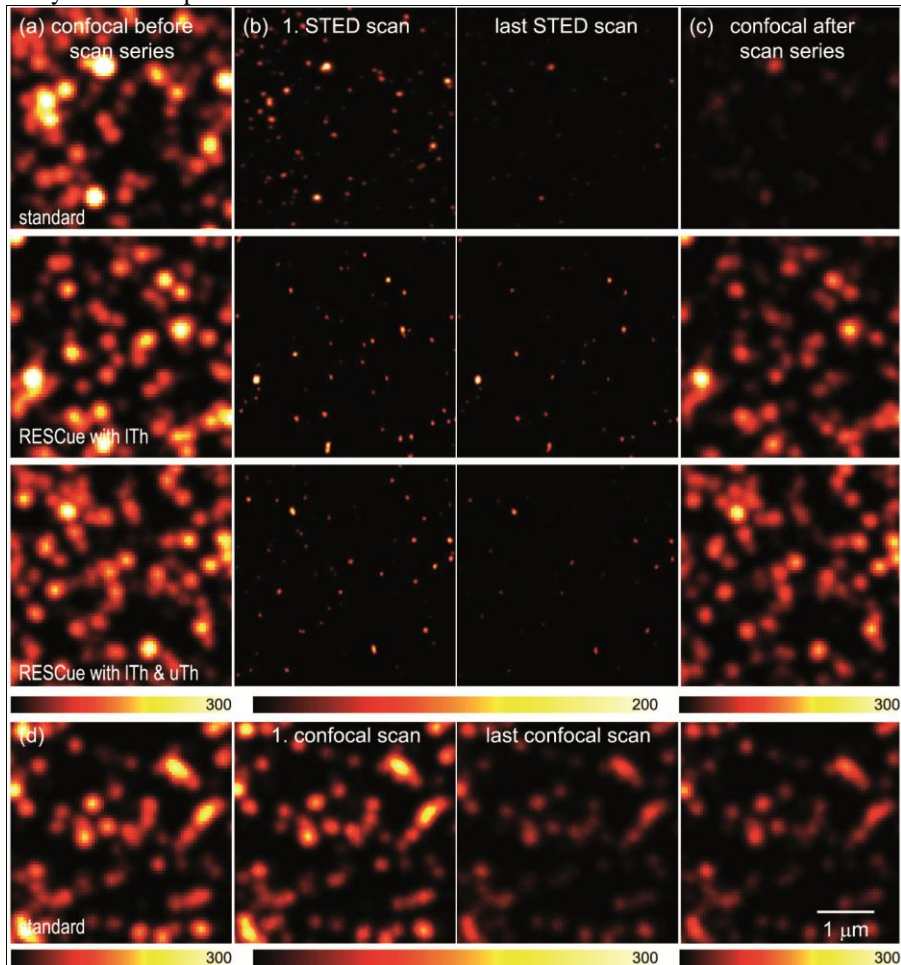


Fig. 3. In RESCue mode bleaching is reduced 5-fold compared to standard STED, exemplified by recording fluorescent beads. (a) and (c) are confocal references taken before and after a series of 10 STED images (b). Each series differs in RESCue settings: (standard) RESCue disabled, (lTh) RESCue with a lower threshold $lTh = 5$ photons and $dT = 50 \mu s$, (lTh&uTh) RESCue with additional upper threshold $uTh = 28$ photons. The pixel dwell time $pT = 400 \mu s$ for all scans. (d) The series with parameter as in (b) with the STED beam switched off show a 20% larger bleach factor than in the RESCue scan with lTh&uTh.

3.1 RESCue-STED of fluorescent beads

Figure 3 shows three scan series of 10 STED images under different RESCue conditions of Nile Red fluorescent nanoparticles. The scan regions were $4 \times 4 \mu m$ in size with a pixel size of $15 \times 15 nm$ and a pixel dwell time of $400 \mu s$. The lTh was set to 5 photons, and $pT = 50 \mu s$. The

uTh parameter was set to 28 photons. The 20 nm sized fluorescent beads appear as sharp dots of 30 nm FWHM in the STED images. That is, compared to the confocal image, a ~7-fold resolution increase in the xy-plane. Photobleaching in the conventional STED mode leads to a 6-fold reduced fluorescence signal after ten scans (Fig. 3b standard). Reducing the excitation and STED light dose by applying RESCue reduces the number of state transitions significantly and therefore the probability of photobleaching. By introducing the lTh, the bleaching factor is reduced by a factor of 4 (Fig. 3b RESCue with lTh). The additional parameter uTh enables a further enhancement in fluorescence signal (Fig. 3a RESCue with lTh & uTh) such that in total the bleaching factor is reduced to 1/5. Performing the same measurement with the STED beam switched off, yields a 20% higher bleaching factor (Fig. 3d standard) rendering the last image in the fourth row dimmer than that of the third row. This shows the potential of exploiting the high resolution information for sample exposure.

3.2 RESCue-STED of labeled proteins: sparse dye distributions benefit from the lower threshold

In the following, we adopted these promising results to biological systems. First we used

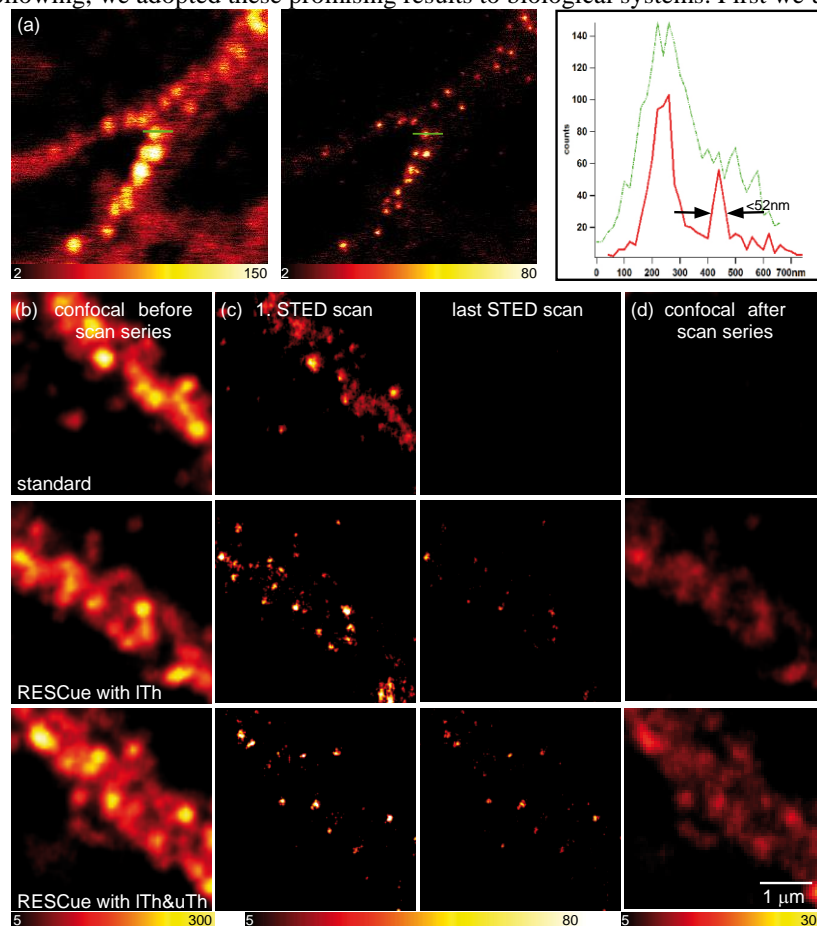


Fig. 4. RESCue reduces photobleaching of Atto565 marked APP proteins in fixed primary mouse neurons by a factor of 4. Confocal image (a, left side) of the APP distribution and STED counterpart (raw data) (a, middle). The line profile reveals 50 nm resolution (a, right side). A confocal image is recorded before (b) and after three STED scans. Without RESCue (c, standard) bleaching precludes data acquisition. RESCue conditions preserve fluorescence better (lTh, lTh&uTh). Parameters: lTh=6 photons, uTh=25 photons and $dT = 40 \mu\text{s}$. Due to the sparse APP distribution the bleaching reduction is dominated by the lTh modality. $pT = 500 \mu\text{s}$ for the confocal and 300 μs for the STED scans.

primary mouse neurons (DIV8) as specimens and immunostained the amyloid precursor protein (APP) with the dye Atto565. The APP is located in the dendritic and axonal compartment of neurons [21]; it is essential for the normal synaptic function and processing, which strongly depend on the intra neuronal localization. APP plays a major role in the etiopathology of Alzheimer's disease the most common form of dementia. Figure 4 shows several scan series of STED images and confocal reference images of the labeled APP located in the plasma membrane. Contrary to the confocal mode STED displays well separated APP clusters (Fig. 4a). The resolution in the STED image is about 50 nm and only limited by the STED beam intensity applied. The confocal images were recorded with 50 nm pixel size and a pixel dwell time of 500 μ s, the three (RESCue-) STED series with a pixel dwell time of 300 μ s and otherwise identical settings as for the images in Fig. 3. We identified a lTh of 6 photons within a dT of 40 μ s to be the best RESCue parameters.

In the case of sparse dye distributions the lTh is rarely reached. Thus the number of transition cycles is minimized primarily by lTh. In contrast for very dense samples for which the lTh is reached at almost all locations the effect of the uTh becomes predominant (see next paragraph and Fig. 5). The comparison to the conventional STED measurement shows a 4-fold reduction in photobleaching. The sparse distribution of APP results in a low photon count rate. Therefore including the upper threshold uTh, which was set to 25 photons, only lead to a minor improvement as expected (Fig. 4c, third row).

3.3 RESCue-STED of labeled GFAP: dense dye distributions benefit from both threshold levels

To demonstrate the effect of RESCue on dense samples we imaged the glial fibrillary protein

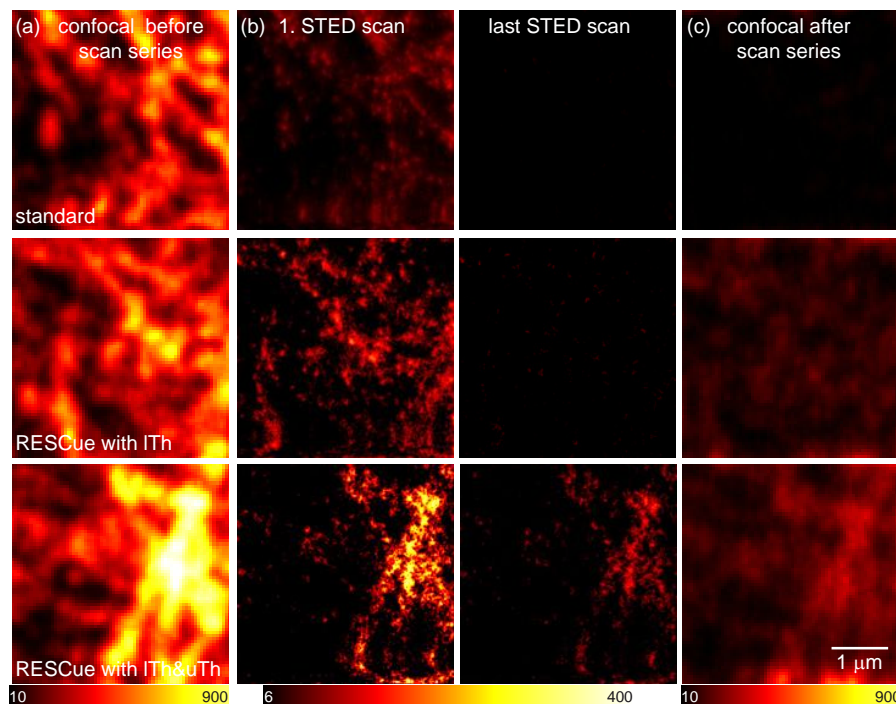


Fig. 5. The parameter uTh further decreases Atto565 bleaching in immunostained glial fibrillary proteins (GFAP) in glioblastoma cells (u373), attaining an overall bleaching reduction factor of 8. Analogous to Fig. 4, the confocal images are recorded before (a) and after (c) a series of three STED scans. Without RESCue, almost all fluorescence was bleached after the third scan (b, *standard*). With a lower threshold lTh of 6 photons and a decision time dT of 40 μ s, the fluorescence of the densely labeled filaments can be preserved for significantly more scans (b, *lTh*). Moreover, with an additional upper threshold uTh of 28 photons, the bleaching reduction can be further improved by a factor of 2 (b, *lTh & uTh*). The pixel dwell time pT was set to 500 μ s for the confocal and 300 μ s for the STED scans.

(GFAP) immunostained with Atto565. Here, the dye molecules are densely packed on a filament, as can be seen in the confocal image (Fig. 5a). All settings were identical to the settings used for imaging APP (Fig. 4) except the uTh was set to 28 photons. In this case, an apparent difference in the bleaching behaviour is not only achieved by introducing the lower threshold (4-fold bleaching reduction), but an additional factor of 2 is attained by adding uTh , resulting in an overall 8-fold reduction in photobleaching. These experiments show that for densely distributed dye molecules fluorescence conservation is further improved by incorporating both threshold parameters.

3.4 RESCue-STED of labeled lamina: RESCue mode facilitates 3D measurements

As discussed in the introduction subdiffraction imaging in 3D requires more transitions than 2D imaging, implying that the maximal number of cycles of typical markers might not be sufficient to record a superresolved image in 3D. By applying or maintaining on-off state gradients only when they are required to separate objects within subwavelength distance, the limited number of cycles can be used more effectively and so enabling applications which demand an extensive number of on-off transitions. Therefore RESCue strategies open up new application areas for coordinate-targeted (RESOLFT-type) 3D-nanoscopy methods. One example is shown in Fig. 6. Here we imaged by STED microscopy Atto647N labeled lamina with a pixel dwell time pT of 100 μs , decision time dT of 30 μs and a value of lTh equalling 426 photons. The 3D data stack was generated by sequential xz scans. The figure shows a 3D surface rendered view of the nuclear lamina. The resolution was < 170 nm in axial direction which is a 3.5-fold improvement in comparison to confocal imaging. On the left hand side the measurement of the standard STED mode is presented. After a few xz -sections the fluorescence capability was lost due to photobleaching.

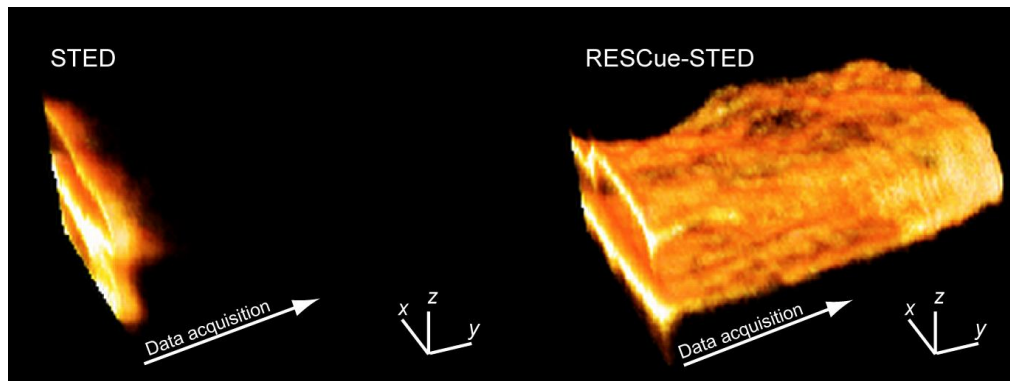


Fig. 6. RESCue allows the measurement of ATTO647N immunostained nuclear lamina in neuroblastoma cells in three dimensions. The left image (STED) shows the attempt to image the lamina without RESCue but fails due to on-off switching fatigue of the fluorophores. Without RESCue the SNR is not sufficient for 3D rendering. The signal is too low and clipped with the background by the 3D reconstruction. An effective use of the limited state transition cycles through RESCue-STED enables 3D subdiffraction imaging (right hand side). The lengths of x , z , y coordinates represent 1 μm , 1 μm and 0.5 μm respectively.

The image on the right hand side shows that under the same conditions, with the aid of RESCue-STED, the fluorescence capability is preserved throughout the 3D imaging. This underscores the feasibility to create 3D data stacks of bleaching prone samples using STED microscopy, which would not be possible without RESCue. Especially 3D applications profit from the RESCue technique because here the ratio between the effective fluorescence volume and the region exposed by the excitation and suppression beams is large due to the third dimension and also due to the elongated shape of the diffraction intensity maxima of the beams along the optical axis.

4. Discussion, conclusion and outlook

We have demonstrated that the reduction of state transition cycles (RESCue) significantly decreases photobleaching in STED microscopy. By avoiding unnecessary transition cycles when there are no objects to be discerned, the limited number of available state transitions is used more economically. The reduction of photobleaching clearly depends both on the fluorophore, the applied intensity, i.e. on the subdiffraction resolution selected according to $\Delta r \approx \lambda / (2n \sin \alpha \sqrt{1 + I/I_s})$, and on the spatial distribution of the fluorophores in the sample.

Therefore, the examples shown in this study can only be exemplary. A 5-fold reduction in photobleaching was demonstrated with imaging beads. An up to 8-fold bleaching reduction is demonstrated for imaging APP labeled neurons and GFAP labeled glial cells, which are practically relevant biological samples. Even in cases where the fluorescence signal is lost completely under standard STED conditions, RESCue enables for example 3D measurements of lamina labeled neuroblastoma cells.

The photon flux measured during a fraction of the pixel dwell time serves as decision criterion of whether a fluorescent object is present in the reduced focal volume. This information is used to reduce the number of optically enforced state transition cycles of the marker molecules as well as the overall light dose without trading off resolution or imaging speed. The implementation of RESCue using a FPGA allows the optimization of the RESCue parameters dT , lTh and uTh during measurements. This helps accounting for changing properties during the measurement by recording an image series. If the sample is heavily bleached during repeated scans in life cell applications, lTh or any other parameter can be adapted accordingly.

This approach is suitable for all 3D far-field optical nanoscopy modalities relying on a targeted coordinate readout (coordinate-targeted state transitions) and reduces all light induced destructive processes due to its efficient use of sample illumination. The highest impact of this method is expected on applications requiring a large number of transition cycles. Examples include extended 3D subdiffraction imaging or when markers are employed affording a very limited number of (on-off) state transitions cycles, such as coumarins or fluorescent proteins.

In the scheme implemented herein (Fig. 1), in order to probe for the presence of a fluorescent feature within the subdiffraction region Δr , at least a single on-off cycle has to be enforced on the neighboring fluorophores. Therefore, the RESCue modality implemented here still involves a single on-off cycle per pixel, meaning that the total number of $m \times m$ cycles stemming from pixel by pixel linear scanning is not reduced by this scheme. Therefore, an alternative way of implementing a RESCue strategy would be to implement a targeted readout mode (i.e. a scanning procedure) that does not initially probe for the presence of a fluorophore, but uses a priori information about its location. In this case one can directly address the coordinates at which fluorescence inhibition is needed and leave out those sites where it would be without function. For example, one could record a lower resolution image first, in order to obtain coarse information about the spatial structure and feature density in the sample. Some features would be rather isolated and some densely packed. One could then (successively) apply a higher spatial resolution and deliberately target regions in which dense features need to be resolved. Concomitantly, one could spare out coordinates in which objects need not be separated and hence no transient switching-off is required. The a priori information about the density of fluorophores or features can be gained from the brightness.

The on-off cycles are not generally identical with the excitation-de-excitation cycles. For example, when employing reversibly photoswitchable fluorescent proteins, or organic fluorophores that are switched by a cis-trans photoisomerization or a change in binding state [6, 7], the optically induced on-off transition can be fully disparate from the excitation/fluorescence generation cycles. However, so far most of the switching processes entailed an action cross-talk between the on-off and fluorescence generation transitions which is why in most cases RESCue strategies also reduce the number of cycles of fluorescence generation as in the method by Manders et al [15]. A similar consideration applies to the

strongly related concept of ground state depletion microscopy [22, 23] whereby the fluorophores are sent to a dark (triplet) state by intense excitation to the fluorescent state followed by occasional intersystem crossing to the dark triplet state. Since both the off-switching and the fluorescence generation are elicited at the same wavelength, action cross-talk is inevitable. In ground state depletion modalities aiming at populating just the fluorescent state, such as saturated structured illumination (SSIM) [24, 25] the situation is related, although the method is more difficult to implement if parallelized schemes using line structured illumination are used.

In STED microscopy action cross-talk of the beams is encountered as well, as can be inferred from the following reasoning. The off-switching of the fluorophore is accomplished by the presence of the STED beam of $I > I_s$, enforcing the fluorophores to dwell in a dark state; only fluorophores that are not subject to the STED beam can spend time in the fluorescent state. The fluorescent state is reached by applying an excitation beam. Therefore, the excitation beam counteracts the off-switching of the dye by the STED beam, thus entangling on-switching and fluorescence read-out. If in the future action cross talk can be avoided in the RESOLFT concept, the saving of on-off transition cycles and of fluorescence generation can be addressed separately, using other decision making criteria on the applications of the beams.

While our strategy aims at minimizing the number of state transitions a fluorophore undergoes during image recording, it is interesting to realize that, most likely, it is not the number of the desired state transitions per se that poses the limitation. For example, there is no particular reason why a fluorophore should not be able to undergo an almost indefinite number of cycles consisting of an excitation to the first excited state by ground state absorption and the reverse de-excitation by stimulated emission from the first excited state back down again. The reason why the number of cycles is correlated with photobleaching is the simple fact that one of the involved states may lead to a bleaching-facilitating state if exposed to one of the involved beams. In the case of STED, bleaching is induced if excited fluorophores are photoexcited to a higher and hence more reactive state, before or after having crossed to the triplet state.

The RESCue strategy is based on the insight that in STED, GSD, RESOLFT, SSIM and related coordinate-targeted on-off switching modalities, subdiffraction resolution is gained by sequentially keeping adjacent molecules or fluorescent features in a state in which they are not able to respond with fluorescence when exposed to excitation light. Because they separate molecules by having them in different states, these concepts are molecule-centered [7]. Therefore, a thorough description of these concepts as well as their optimization cannot rely on a formalisms dealing just with wave propagation. In fact, in all relevant fluorescence superresolution methods, no matter if the method operates in the stochastic single molecule or in the coordinate-targeted on-off switching mode like STED microscopy, the fluorophores and their (on-off) transitions are at the center stage [6, 7]. For this reason, contrary to a recent article contesting this description [26], in all established superresolution or fluorescence nanoscopy methods, no matter if stochastic (PALM [3], STORM [4], GSDIM [27,28]) or coordinate-targeted (STED, GSD [22, 23], SSIM [24], RESOLFT [29]) the object cannot be viewed as 'continuous'. The results demonstrated in this paper highlight this fundamental fact for STED, just as they underscore that understanding the on-off molecular transition as the enabling element directly leads to a method improvement. By resolving fluorophores or fluorescent features through making them distinct by their states, all these superresolution methods inherently rest on the granularity of molecules.

In any case, the reduced photobleaching realized by a RESCue strategy can be reinvested in higher resolution and/or longer acquisition times allowing for repeated scans which are a prerequisite for studying dynamical processes under live cell conditions. As a side effect, RESCue is also helpful for reducing phototoxicity. For all these reasons, we expect RESCue to become important for all RESOLFT type nanoscopy modalities and STED microscopy in particular.

Acknowledgements

The authors thank S. Back and S. Kins (ZMBH, Heidelberg) for supplying the mouse embryonic neurons and Jay Jethwa for critical reading. We also acknowledge Picoquant (Berlin, Germany) for kindly providing the PicoTA 530 laser.